

Three New Co(II)/Ni(II) Coordination Polymers Based on 3,3'-biphenyl Dicarboxylic Acid and N-donor Co-ligands: Synthesis, Crystal Structures and Magnetic Properties¹

H. B. Wang^a, Y. P. Wu^b, *, G. W. Xu^b, J. F. Wang^b, and S. S. Guo^b

^aCollege of Mechanical & Power Engineering, China Three Gorges University, Yichang, 443002 P.R. China

^bCollege of Materials & Chemical Engineering, China Three Gorges University, Yichang, 443002 P.R. China

*e-mail: wyapan2008@163.com

Received February 10, 2015

Abstract—Three new Co(II)/Ni(II) coordination polymers $[\text{Co}(\text{Bpdc})(\text{Bipy})]_n$ (**I**) and $[\text{Co}_2(\text{Bpdc})_2(\text{Dps})_2]_n$ (**II**) and $[\text{Ni}(\text{Bpdc})(\text{Dps})]_n$ (**III**) (H_2Bpdc = 3,3'-biphenyl dicarboxylic acid, Bipy = 2,2'-bipyridine, and Dps = 4,4'-dipyridyl sulfide) have been synthesized via hydrothermal method and characterized by elemental analysis, FT-IR, PXRD and single-crystal X-ray diffraction (CIF files CCDC nos. 994521 (**I**), 994522 (**II**), 1027995 (**III**)). Compound **I** is a 3D supramolecular structures extending through 1D double chain by the $\pi\cdots\pi$ stack interactions. However, compound **II** and **III** are topological isomorphic, which features a 3D four-fold interpenetrated networks with 4-connected dia topology. Moreover, thermogravimetric analysis and magnetic properties of **I** and **II** were also discussed.

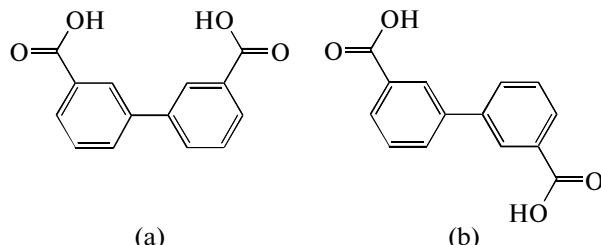
DOI: 10.1134/S1070328415100097

INTRODUCTION

Recently, there are a great of interests which are focused on the synthesis, crystal structure and properties study of metal-organic frameworks for their potential application in the field of luminescence, magnetism, catalyst and so on [1–9]. In this context, the rational design and synthesis diverse structural topologies with specific functions are always of great challenge for the chemists. In order to solve this problem, the action of organic building blocks with polytropic configurations has been investigated in the process of assembling MOFs. It is well known that the aromatic polycarboxylates are widely used in the construction of coordination polymers because of their diverse coordination modes [10–13]. Among these, 4,4'-biphenyl dicarboxylic acid, 3,4'-biphenyl dicarboxylic acid, and 3,3'-biphenyl dicarboxylic acid (H_2Bpdc), have extensively employed to construct many coordination polymers with different strutures and properties due to their flexible coordination modes [14–18]. Furthermore, the N-containing ligands, such as pyridine and imidazole derivatives, have supper coordinaiton property on transition metal ions, and they have different function in the construction of MOFs [19–21].

In our prvious work, two Zn(II) and Cd(II) coordination compounds based on H_2Bpdc (Scheme 1) have been obtained and characterized [22]. Two possible geometrical configurations of H_2Bpdc ligand: *cis*-

configuration (a), *trans*-configuration (b) are in Scheme 1.



Scheme 1.

In order to do further investigation on the vrtial coordination mode of H_2Bpdc and the synergic action between the Bpdc ligand and bipyridyl derivates, herein, three new Co(II)/Ni(II) coordination polymers, namely $[\text{Co}(\text{Bpdc})(\text{Bipy})]_n$ (**I**), $[\text{Co}_2(\text{Bpdc})_2(\text{Dps})_2]_n$ (**II**), and $[\text{Ni}(\text{Bpdc})(\text{Dps})]_n$ (**III**) (Bipy = 2,2'-bipyridine, Dps = 4,4'-dipyridyl sulfide) have been successfully synthesized and characterized. Moreover, the thermal stability and magnetic properties of compounds **I** and **II** has also been investigated.

EXPERIMENTAL

Materials and instrumentation. The organic ligands employed were received from Alfa Aesar and other in-

¹ The article is published in the original.

organic salt and solvents were received as reagent grade and used without any further purification. Elemental analyses were performed with a PerkinElmer 2400 Series II analyzer. The IR spectra were measured as KBr pellets with a FT-IR Nexus spectrophotometer from 4000 to 400 cm^{-1} . Powder X-ray diffractions (PXRD) patterns were recorded on a Rigaku Ultima IV diffractometer with $\text{Cu}K\alpha$ radiation ($\lambda = 1.5406 \text{ \AA}$). The simulated powder patterns were calculated using Mercury 1.4. The purity and homogeneity of the bulk products were determined by comparison of the simulated and experimental X-ray powder diffraction patterns. Thermogravimetric analysis (TGA) was taken with a NETZSCH STA 449C microanalyzer in under an air atmosphere at a heating rate of $10^\circ\text{C min}^{-1}$. Variable-temperature magnetic measurements were carried out on a Quantum Design SQUID MPMS XL-7 instrument in the magnetic field of 1 kOe, and the diamagnetic corrections were evaluated using Pascal's constants.

Synthesis of compound I. A mixture of $\text{Co}(\text{NO}_3)_2 \cdot 6\text{H}_2\text{O}$ (29.7 mg, 0.10 mmol), 3,3'- H_2Bpdc (24.2 mg, 0.10 mmol), 2,2'-Bipy (15.6 mg, 0.10 mmol), and NaOH (8.0 mg, 0.20 mmol) in a solution of H_2O (7 mL) were sealed into a 23 mL Teflon-lined stainless steel container under autogenous pressure, heated at 140°C for 3 days and cooled to room temperature for 24 h. Purple prismatic single crystals suitable for X-ray analyses were obtained. The yield was 67% (based on Co(II)).

For $\text{C}_{24}\text{H}_{16}\text{N}_2\text{O}_4\text{Co}$

anal. calcd., %: C, 63.31; H, 3.54; N, 6.15.
Found., %: C, 63.22; H, 3.49; N, 6.23.

IR (KBr pellet; ν, cm^{-1}): 2968 w, 1606 w, 1560 m, 1542 s, 1473 w, 1441 m, 1419 s, 1385 m, 1361 s, 1269 w, 1157 w, 1081 w, 1022 w, 904 w, 863 w, 757 s.

Synthesis of compound II was carried out in a similar method used for I except that Bipy was replaced by Dps (18.8 mg, 0.10 mmol). The yield was 43% (based on Co(II)).

For $\text{C}_{48}\text{H}_{32}\text{N}_4\text{O}_8\text{S}_2\text{Co}_2$

anal. calcd., %: C, 59.14; H, 3.31; N, 5.75.
Found., %: C, 59.35; H, 3.53; N, 5.83.

IR (KBr pellet; ν, cm^{-1}): 3217 w, 1589 m, 1534 m, 1481 w, 1413 s, 1372 m, 1266 w, 1183 w, 1057 w, 1022 w, 862 w, 830 w, 812 w, 793 m, 760 s, 732 m.

Synthesis of compound III was carried out in a similar method to that of II. The yield was 38% (based on Ni(II)).

For $\text{C}_{24}\text{H}_{16}\text{N}_2\text{O}_4\text{Sn}$

anal. calcd., %: C, 59.17; H, 3.31; N, 5.75.
Found., %: C, 59.25; H, 3.27; N, 5.93.

IR (KBr pellet; ν, cm^{-1}): 3445 m, 2922 w, 2981 w, 1622 s, 1584 s, 1540 m, 1480 w, 1409 s, 1384 s, 1315 w, 1213 w, 828 w, 756 m.

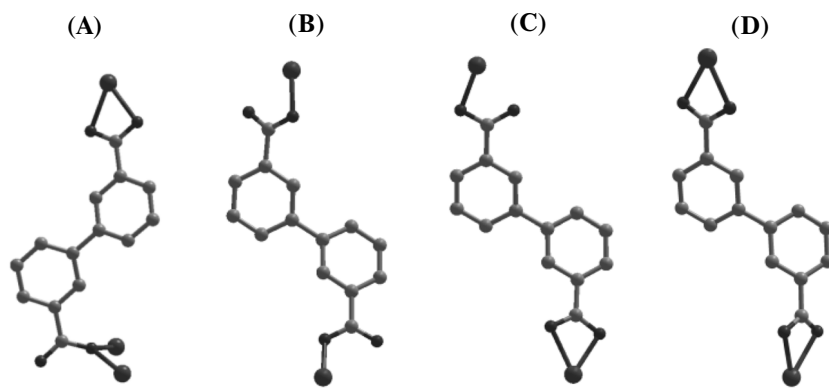
X-ray structure determination. Single crystal X-ray diffraction analysis of compounds I–III were carried out on a Rigaku XtaLAB mini diffractometer with graphite monochromated $\text{Mo}K\alpha$ radiation ($\lambda = 0.71073 \text{ \AA}$). The collected data were reduced using the program CRYSTALCLEAR and an empirical absorption correction was applied [23]. The structure was solved by direct methods and refined based on F^2 by the full matrix least-squares methods using SHELXTL [24, 25]. The hydrogen atoms were assigned with common isotropic displacement factors and included in the final refinement by use of geometrical restraints. Generally, the positions of C/N-bound H atoms were generated by a riding model on idealized geometries. The crystallographic data for I–III are listed in Table 1 and selected bond lengths and angles are given in Table 2.

The supplementary crystallographic data for I–III been deposited the Cambridge Crystallographic Data Centre (CCDC nos. 994521 (I), 994522 (II), 1027995 (III); deposit@ccdc.cam.ac.uk or <http://www.ccdc.cam.ac.uk>).

RESULTS AND DISCUSSION

Single crystal structure analysis shows that the asymmetric unit of compound I consists of one Co^{2+} ion, one Bpdc and one Bipy ligand. Each Co^{2+} ion is six-coordinated by two nitrogen donors (N(1) and N(2)) from one bipy ligand and four carboxylate oxygen donors (O(1), O(2), O(3)^{#1} and O(3)^{#2}, symmetry codes: ^{#1} $x - 1, y, z + 1$; ^{#2} $-x + 1, -y + 1, -z$) from three 3,3'-Bpdc ligands, thus generating an octahedral geometrical configuration (Fig. 1). The coordination Co–O/N bonds, varying from 2.344(3) to 2.608(3) \AA , are within the reported results [26].

Four coordination modes of Bpdc in I–III: $\mu_3\text{-}\eta^1\text{:}\eta^1\text{:}\eta^2$ (A); $\mu_2\text{-}\eta^1\text{:}\eta^1$ (B); $\mu_2\text{-}\eta^1\text{:}\eta^1\text{:}\eta^1$ (C); $\mu_2\text{-}\eta^1\text{:}\eta^1\text{:}\eta^1\text{:}\eta^1$ (D) are given in Scheme 2:



Scheme 2.

Table 1. Crystallographic data and structure refinement information for compounds **I**–**III**

Parameter	Value		
	I	II	III
Formula weight	455.32	974.76	487.16
Temperature (K)	296(2)	296(2)	296(2)
Crystal system	Triclinic	Monoclinic	Orthorhombic
Space group	$P\bar{1}$	$P2_1/c$	$Pbca$
Unit cell dimensions			
<i>a</i> , Å	10.173(6)	17.409(7)	17.7833(3)
<i>b</i> , Å	10.396(6)	11.827(5)	11.9359(2)
<i>c</i> , Å	11.940(7)	20.220(8)	19.3104(3)
α , deg	72.60(3)	90	90
β , deg	66.70(3)	92.757(6)	90
γ , deg	61.04(3)	90	90
Volume, Å ³ ; <i>Z</i>	1005.6(10); 2	4158(3); 4	4098.82; 8
ρ_{calcd} , mg/m ³	1.504	1.557	1.579
$\mu(\text{MoK}\alpha)$, mm ⁻¹	0.888	0.961	1.085
<i>F</i> (000)	466	1992	2000
θ Range, deg	2.45–27.53	3.02–27.46	2.11–27.56
Limiting indices	$-13 \leq h \leq 13$ $-13 \leq k \leq 13$ $-15 \leq l \leq 15$	$-22 \leq h \leq 22$ $-15 \leq k \leq 15$ $-26 \leq l \leq 26$	$-20 \leq h \leq 23$ $-15 \leq k \leq 13$ $-19 \leq l \leq 25$
Crystal size, mm	0.23 × 0.21 × 0.16	0.16 × 0.14 × 0.10	0.18 × 0.16 × 0.15
Relections collected	10724	43410	19106
Independent reflection (R_{int})	4607 (0.0730)	9496 (0.0894)	4736 (0.0274)
Data/restraints/parameters	4607/0/280	9496/0/577	4736/0/289
Goodness-of-fit on F^2	1.011	1.098	1.021
R_1^* , wR_2^{**} ($I > 2\sigma(I)$)	0.0595, 0.1642	0.0538, 0.1114	0.0328, 0.0838
R_1^* , wR_2^{**} (all data)	0.0719, 0.1727	0.0750, 0.1219	0.0492, 0.0927
$\Delta\rho_{\text{max}}/\Delta\rho_{\text{min}}$, e Å ⁻³	1.212/–0.880	0.549/–0.497	0.341/–0.428

* $R_1 = \sum(|F_0| - |F_c|)/\sum|F_0|$; ** $wR_2 = \{\sum[w(|F_0|^2 - |F_c|^2)^2]/\sum[w(|F_0|^2)^2]\}^{1/2}$.

Table 2. The selected bond lengths (Å) and bond angles(deg) for **I**–**III***

I			
Bond	<i>d</i> , Å	Bond	<i>d</i> , Å
Co(1)–O(3) ^{#1}	2.034(3)	Co(1)–N(1)	2.130(3)
Co(1)–O(3) ^{#2}	2.117(2)	Co(1)–O(1)	2.171(3)
Co(1)–N(2)	2.129(3)	Co(1)–O(2)	2.172(3)
Angle	ω, deg	Angle	ω, deg
O(3) ^{#1} Co(1)O(3) ^{#2}	79.24(10)	N(2)Co(1)O(1)	90.82(12)
O(3) ^{#1} Co(1)N(2)	96.90(11)	N(1)Co(1)O(1)	153.31(11)
O(3) ^{#2} Co(1)N(2)	172.40(10)	O(3) ^{#1} Co(1)O(2)	159.91(10)
O(3) ^{#1} Co(1)N(1)	102.75(11)	O(3) ^{#2} Co(1)O(2)	91.34(10)
N(2)Co(1)N(1)	76.60(12)	N(2)Co(1)O(2)	94.29(12)
O(3) ^{#1} Co(1)O(1)	102.07(10)	N(1)Co(1)O(2)	96.04(11)
O(3) ^{#2} Co(1)O(1)	96.38(11)	O(1)Co(1)O(2)	61.05(10)

II			
Bond	<i>d</i> , Å	Bond	<i>d</i> , Å
Co(1)–O(1)	2.027(2)	Co(2)–O(3) ^{#2}	1.940(3)
Co(1)–N(2) ^{#1}	2.087(2)	Co(2)–O(7)	2.000(2)
Co(1)–N(1)	2.105(3)	Co(2)–N(3)	2.051(3)
Co(1)–O(5)	2.121(2)	Co(2)–N(4) ^{#3}	2.083(2)
Co(1)–O(6)	2.189(2)	Co(1)–O(1)	2.027(2)
Angle	ω, deg	Angle	ω, deg
O(1)Co(1)N(2) ^{#1}	106.97(10)	O(5)Co(1)O(6)	61.00(9)
O(1)Co(1)N(1)	92.57(10)	O(3) ^{#2} Co(2)O(7)	121.85(12)
N(2) ^{#1} Co(1)N(1)	101.94(10)	O(3) ^{#2} Co(2)N(3)	100.06(12)
O(1)Co(1)O(5)	141.15(9)	O(7)Co(2)N(3)	116.08(10)
N(2) ^{#1} Co(1)O(5)	97.82(9)	O(3) ^{#2} Co(2)N(4) ^{#3}	121.92(11)
N(1)Co(1)O(5)	111.28(10)	O(7)Co(2)N(4) ^{#3}	93.17(10)
O(1)Co(1)O(6)	90.30(10)	N(3)Co(2)N(4) ^{#3}	103.46(10)
N(2) ^{#1} Co(1)O(6)	158.64(10)	N(2) ^{#1} Co(1)O(5)	97.82(9)
N(1)Co(1)O(6)	89.44(10)		

III			
Bond	<i>d</i> , Å	Bond	<i>d</i> , Å
Ni(1)–N(1)	2.0512(15)	Ni(1)–O(1)	2.0566(14)
Ni(1)–O(3) ^{#1}	2.0697(13)	Ni(1)–N(2) ^{#2}	2.0890(17)
Ni(1)–O(4) ^{#1}	2.1508(15)	Ni(1)–O(2)	2.2250(15)
Angle	ω, deg	Angle	ω, deg
N(1)Ni(1)O(1)	102.91(6)	N(1)Ni(1)O(3) ^{#1}	160.65(6)
O(1)Ni(1)O(3) ^{#1}	94.24(5)	N(1)Ni(1)N(2) ^{#2}	97.09(6)
O(1)Ni(1)N(2) ^{#2}	89.64(6)	O(3) ^{#1} Ni(1)N(2) ^{#2}	91.84(6)
N(1)Ni(1)O(4) ^{#1}	98.46(6)	O(1)Ni(1)O(4) ^{#1}	150.34(6)
O(3) ^{#1} Ni(1)O(4) ^{#1}	62.37(5)	N(2) ^{#2} Ni(1)O(4) ^{#1}	107.97(6)
N(1)Ni(1)O(2)	91.28(6)	O(1)Ni(1)O(2)	61.29(5)
O(3) ^{#1} Ni(1)O(2)	89.15(6)	N(2) ^{#2} Ni(1)O(2)	150.89(6)
O(4) ^{#1} Ni(1)O(2)	98.21(6)		

* Symmetry codes: ^{#1} $x - 1, y, z + 1$; ^{#2} $-x + 1, -y + 1, -z$ (**I**); ^{#1} $x, -y + 1/2, z + 1/2$; ^{#2} $x + 1, y, z$; ^{#3} $x, -y + 5/2, z - 1/2$ (**II**); ^{#1} $x - 1/2, -y + 3/2, -z$; ^{#2} $x, -y + 5/2, z - 1/2$ (**III**).

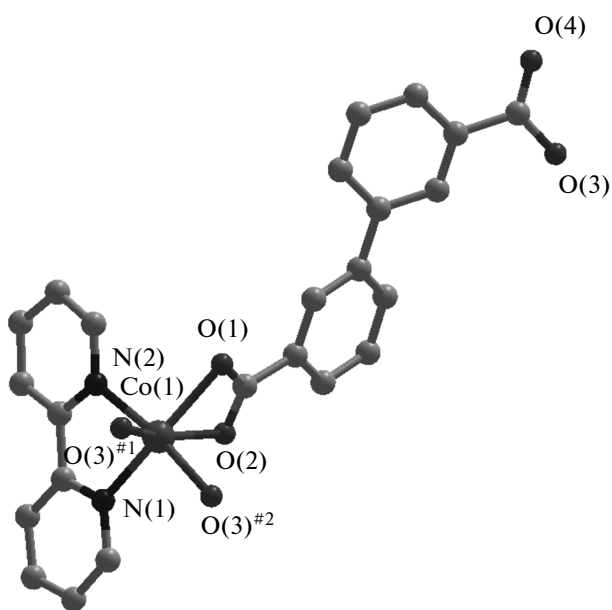


Fig. 1. The coordination environment of Co(II) in **I**. Symmetry codes: ${}^{\#1}x-1, y, z+1$; ${}^{\#2}-x+1, -y+1, -z$.

In **I**, the adjacent Co^{2+} ions are linked by two Bpdc ligands with the $\mu_3\text{-}\eta^1\text{:}\eta^1\text{:}\eta^2$ (type A; Scheme 2), which result in the 1D double chain structures along the z axis (Fig. 2a). These chains extended into the 2D layer in the xy plane *via* the $\pi\cdots\pi$ stack interaction of pyridyl ring (centroid-to-centroid distance is 3.729 Å) (Fig. 2b). Furthermore, the 2D layers are linked into 3D supramolecular structure by the little weaker $\pi\cdots\pi$ interaction of aromatic rings of Bpdc ligands between adjacent layers (3.757 Å) (Fig. 2c and Fig. 2d).

Compounds **II** and **III** are topological isomorphic, which exhibits a 3D four-fold interpenetrated networks with 4-connected **dia** topology. Structural analysis reveals that two complexes crystallize in different crystal system and space groups and display same 4-connected **dia** topological skeletons. The asymmetric unit of **II** contains two crystallographically unique Co^{2+} ions, two Bpdc²⁻ anions and two Dps ligands (Fig. 3a). The $\text{Co}(1)$ ion shows a distorted octahedral coordination geometry $[\text{CoN}_2\text{O}_4]$, which is completed by three carboxylate oxygen atoms (O(1), O(5) and O(6)) from two different Bpdc²⁻ anions and two nitrogen atoms (N(1) and N(2)^{#1}), symmetry codes: ${}^{\#1}x, -y+1/2$,

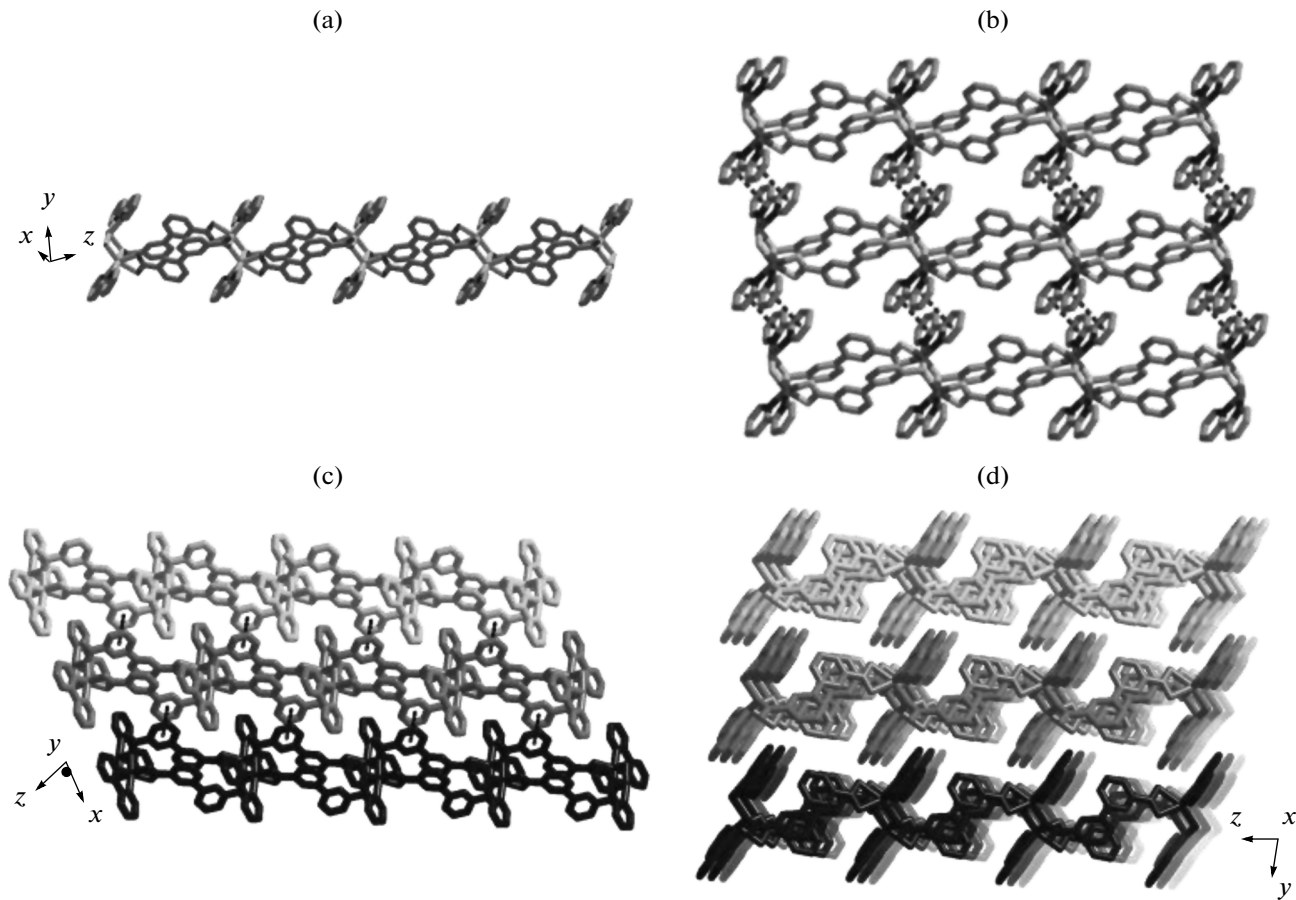


Fig. 2. View of the 1D double chain along the z axis (a); the 2D layer constructed by 1D double chain *via* the $\pi\cdots\pi$ interaction (b); the adjacent layers *via* the weak interaction (c); the packing 3D supramolecular structures of **I** (d).

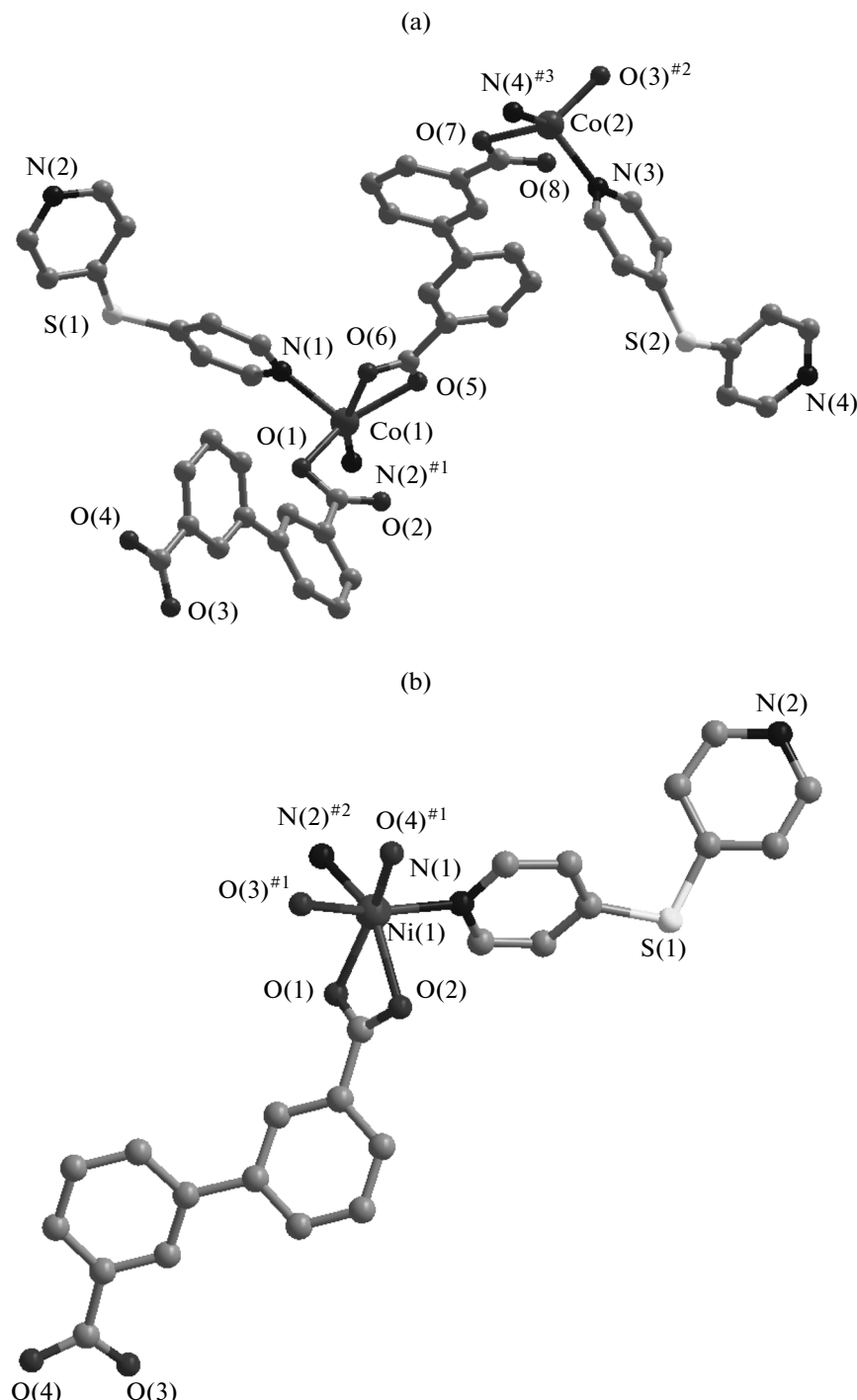


Fig. 3. The coordination environment center of Co(II) in **II** (a) and Ni(II) in **III** (b). Symmetry codes: ^{#1} x, -y + 1/2, z + 1/2; ^{#2} x + 1, y, z; ^{#3} x, -y + 5/2, z - 1/2 (II); ^{#1} x - 1/2, -y + 3/2, -z; ^{#2} x, -y + 5/2, z - 1/2.

$z + 1/2$) from two different Dps molecules. The Co(2) ion is coordinated in a distorted tetrahedral geometry $[\text{CoN}_2\text{O}_2]$ by two O atoms (O(3)^{#2} and O(7), symmetry codes: ^{#2} x + 1, y, z) from the monodentate carboxylate groups of two Bpdc²⁻ anions and two nitrogen atoms (N(3) and N(4)^{#3}, symmetry codes: ^{#3} x, -y + 5/2,

$z - 1/2$) from two Dps molecules. Different from compound **I**, the asymmetric unit of **III** contains one crystallographically unique Ni²⁺ ions, one Bpdc²⁻ anions and one Dps ligand (Fig. 3b). The central Ni²⁺ ion shows an obviously distorted octahedral coordination geometry $[\text{NiN}_2\text{O}_4]$, which is ligated by four carboxy-

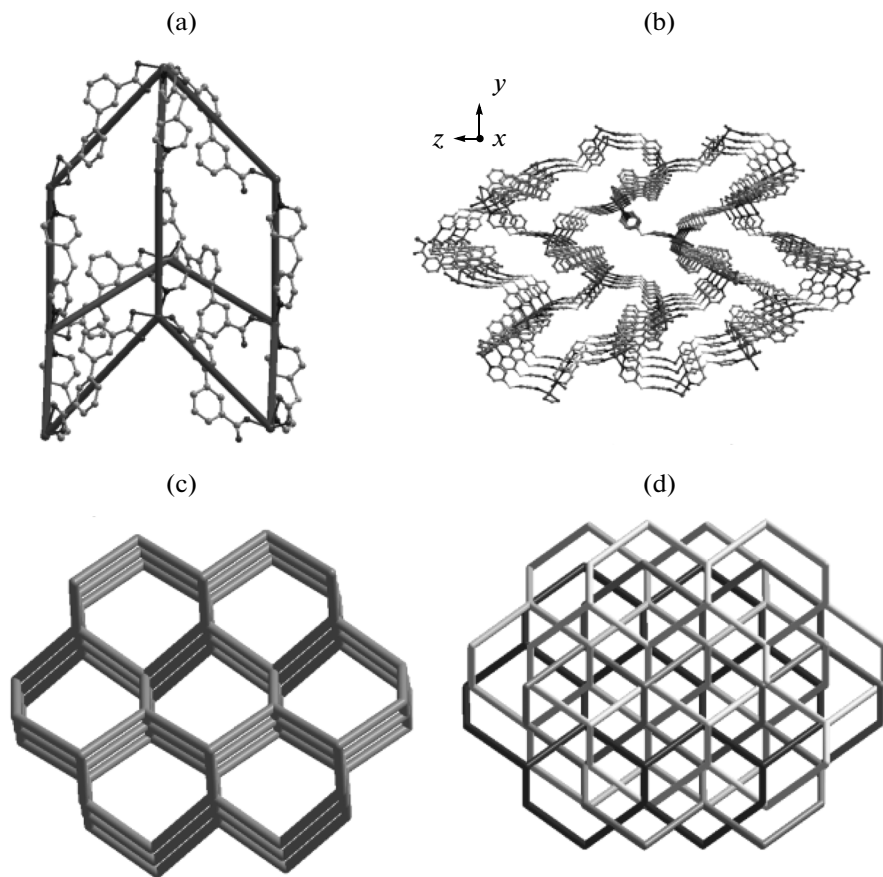


Fig. 4. Topological view showing the adamantane unit network in **II** (a); view of the complicated 3D frameworks containing 1D channels with the size of $22.67 \times 11.65 \text{ \AA}^2$ along the x axis (b); the single 3D net with dia topology (c); schematic description of f -fold interpenetrating topology net of **II** (d).

late oxygen atoms ($\text{O}(1)$, $\text{O}(2)$, $\text{O}(3)^{\#1}$ and $\text{O}(4)^{\#1}$, symmetry codes: $^{\#1} x -1/2, -y + 3/2, -z$) from two different Bpdc^{2-} anions and two nitrogen atoms ($\text{N}(1)$

and $\text{N}(2)^{\#2}$, symmetry codes: $^{\#2} x, -y + 5/2, z - 1/2$) from two different dps molecules. And the $\text{Co}/\text{Ni}-\text{O}/\text{N}$ bond lengths and angles all are comparable with those reported in the Co/Ni -based compounds [27].

It is noted that the 3,3'-Bpda ligands display three different coordination modes: $\mu_2\text{-}\eta^1\text{:}\eta^1$ (Type **B**; Scheme 2 for **II**) and $\mu_2\text{-}\eta^1\text{:}\eta^1\text{:}\eta^1$ (Type **C**; Scheme 2 for **II**) and $\mu_2\text{-}\eta^1\text{:}\eta^1\text{:}\eta^1$ (Type **D**; Scheme 2 for **III**), respectively. Simultaneously, the dps ligands compensate for the need of metal coordination numbers as well as stabilize the resulting 3D network. Thus, the $\text{Co}(\text{II})/\text{Ni}(\text{II})$ centers are connected by two types of spacers to generate a typical (6.3) net (Fig. 4a). The other 3,3'-Bpda $^{2-}$ anion further extends the (6.3) nets into a 3D dia framework (Fig. 4b and Fig. 4c). It has been well-known that diamond networks tend to interpenetrate to fill the voids within a single net. In **II** and **III**, notably, the (6.3) nets are pillared by the 3,3'-Bpda $^{2-}$ anions, thus resulting in a large hexagonal channel with the size $22.67 \times 11.65 \text{ \AA}^2$, which allows other four selfsame dia nets to penetrate and thus, affords a four-fold interpenetrating framework along the y axis (Fig. 4d).

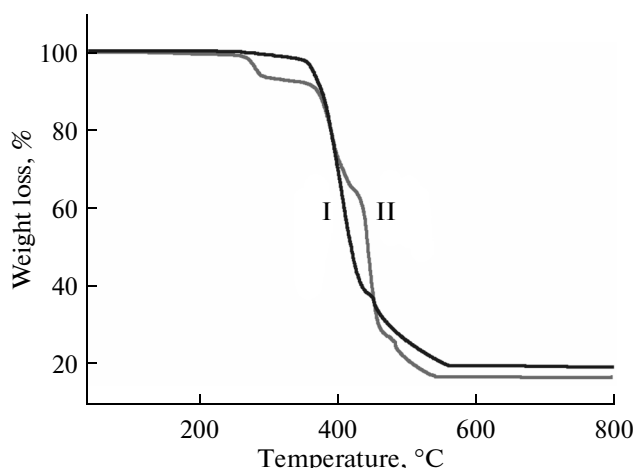


Fig. 5. The TG curves of compound **I** and **II**.

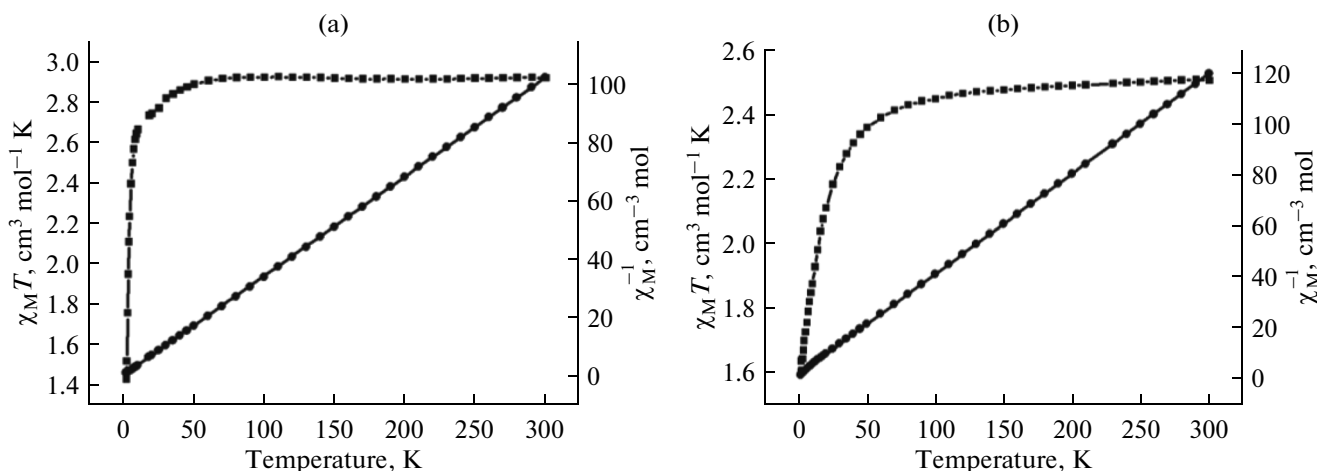


Fig. 6. Temperature dependence of the $\chi_M T$ and χ_M^{-1} curves of I (a) and II (b).

PXRD was used to check the purity of **I** and **II** at room temperature. All the peaks displayed in the measured patterns for each compound closely match those in the simulated patterns generated from single-crystal diffraction data, indicating that the single phases of **I** and **II** were formed. The TGA curves of **I**–**III** are similar and exhibit one main step of weight loss corresponding to the combustion of the organic groups. Therefore, only the patterns of **I** and **II** will be discussed as an example. As shown in Fig. 5, **I** and **II** are thermally stable to 350 and 270°C, respectively. Thereafter significant weight loss occurs resulting in complete decomposition of the compounds. The residues indicate that the final products are the metal oxides.

The variable-temperature magnetic susceptibility (χ_M) data for **I** and **II** were collected over the temperature range of 2–300 K under an applied field of 1 kOe (Fig. 6). At room temperature, the $\chi_M T$ values of **I** and **II** at 300 K are 2.92 and 2.50 $\text{cm}^3 \text{mol}^{-1} \text{K}$, which were slightly smaller than that of two isolated spin-only Co^{2+} ions ($3.75 \text{ cm}^3 \text{ mol}^{-1} \text{K}$) and larger than one isolated spin-only Co^{2+} cations ($1.88 \text{ cm}^3 \text{ mol}^{-1} \text{K}$) in the asymmetric unit, respectively. Upon cooling, the $\chi_M T$ value of **I** and **II** both decrease monotonically, reaching a minimum of $1.52 \text{ cm}^3 \text{ mol}^{-1} \text{K}$ for **I** and $1.60 \text{ cm}^3 \text{ mol}^{-1} \text{K}$ for **II** at 2 K, indicating overall anti-ferromagnetic interactions of **I** and **II**. The temperature dependence of the reciprocal susceptibility of ($1/\chi_M$) of **I** and **II** obey the Curie–Weiss law. Fitting the curve of **I** and **II** give parameters $\theta = -1.06 \text{ K}$, $C = 2.93 \text{ cm}^3 \text{ K mol}^{-1}$ for **I** and $\theta = -3.04 \text{ K}$, $C = 2.53 \text{ cm}^3 \text{ K mol}^{-1}$ for **II**. The negative θ value demonstrate that in both of **I** and **II** there exist anti-ferromagnetic interaction between the adjacent Co^{2+} ions mediated through the carboxylate bridges, which is comparable to those reported for other similar Co(II) compounds [26, 28].

ACKNOWLEDGMENTS

This work was financially supported by the NSF of China (no. 21373122), the NSF of Hubei Provinces of China (no. 2014CFB277), the NSRF of Hubei Provincial Education Office of China (Q20141201) and the SRASF of Yichang of Hubei Province (A13-302a-02).

REFERENCES

1. Du, M., Li, C.P., Liu, C.S., and Fang, S.M., *Coord. Chem. Rev.*, 2013, vol. 257, p. 1282.
2. Yang, G.P., Hou, L., Luan, X.J., et al., *Chem. Soc. Rev.*, 2012, vol. 41, p. 6992.
3. Yang, G.P., Hou, L., Ma, L.F., and Wang, Y.Y., *CrystEngComm.*, 2013, vol. 15, p. 2561.
4. Liu, J.Q., Wu, J., Jia, Z.B., et al., *Dalton Trans.*, 2014, vol. 43, p. 17265.
5. Li, D.S., Wu, Y.P., Zhao, J., et al., *Coord. Chem. Rev.*, 2014, vol. 261, p. 1.
6. Kuppler, R.J., Timmons, D.J., Fang, Q.R., et al., *Coord. Chem. Rev.*, 2009, vol. 253, p. 3042.
7. Farha, O.K., Wilmer, C.E., Eryazici, I., et al., *J. Am. Chem. Soc.*, 2012, vol. 134, p. 9860.
8. McDonald, T.M., Lee, W.R., Mason, J.A., et al., *J. Am. Chem. Soc.*, 2012, vol. 134, p. 7056.
9. Wilmer, C.E., Leaf, M., Lee, C.Y., et al., *Nat. Chem.*, 2012, vol. 4, p. 83.
10. Li, D.S., Wu, Y.P., Zhang, P., et al., *Cryst. Growth Des.*, 2010, vol. 10, p. 2037.
11. Li, D.S., Zhang, P., Zhao, J., et al., *Cryst. Growth Des.*, 2012, vol. 12, p. 1697.
12. Li, G.L., Liu, G.Z., Ma, L.F., et al., *Chem. Commun.*, 2014, vol. 50, p. 2615.
13. Gai, Y., Jiang, F., Chen, L., et al., *Cryst. Growth Des.*, 2014, vol. 14, p. 1010.
14. Niu, C.Y., Zheng, X.F., Wan, X.S., and Kou, C.H., *Cryst. Growth Des.*, 2011, vol. 11, p. 2874.

15. Niu, C.Y., Pan, Z.L., Dang, Y.L., et al., *J. Inorg. Organomet. Polym. Mater.*, 2011, vol. 21, p. 611.
16. Jia, W., Luo, J., and Zhu, M., *Cryst. Growth Des.*, 2011, vol. 11, p. 2386.
17. Li, T., Wang, F.L., Wu, S.T., et al., *Cryst. Growth Des.*, 2013, vol. 13, p. 3271.
18. Zhang, C., Zhang, M., Qin, L., and Zheng, H., *Cryst. Growth Des.*, 2013, vol. 14, p. 491.
19. Wu, Y.P., Li, D.S., Fu, F., et al., *Cryst. Growth Des.*, 2011, vol. 11, p. 3850.
20. Zhao, J., Li, D.S., Wu, Y.P., et al., *Inorg. Chem. Commun.*, 2013, vol. 35, p. 61.
21. Burrows, A.D., Jurcic, M., Keenan, L.L., et al., *Chem. Commun.*, 2013, vol. 49, p. 11260.
22. Mu, Y.Q., Zhu, B.F., Li, D.S., et al., *Inorg. Chem. Commun.*, 2013, vol. 33, p. 86.
23. Rigaku, *CrystalClear, Version 2.0*, Tokyo (Japan): Rigaku Corporation, 2009.
24. Sheldrick, G.M., *SHELXS-97, Program for the Solution of Crystal Structures*, Göttingen (Germany): Univ. of Göttingen, 1997.
25. Sheldrick, G.M., *SHELXL, Program for the Refinement of Crystal Structures*, Göttingen (Germany): Univ. of Göttingen, 1997.
26. Li, D.S., Zhao, J., Wu, Y.P., et al., *Inorg. Chem.*, 2013, vol. 52, p. 8091.
27. Chang, X.H., Qin, J.H., Ma, L.F., et al., *Cryst. Growth Des.*, 2012, vol. 12, p. 4649.
28. Zhao, J., Li, D.S., Ke, X.J., et al., *Dalton Trans.*, 2012, vol. 41, p. 2560.L